

## 9 Stability of the Spherical Shape

### 9.1 Rotational But Not Spherical Symmetry?

Ever so often we observe that a balloon, which is spherical in the undistorted state, becomes elongated upon inflation so that we obtain a rotationally symmetric ellipsoid-like shape with the axis of rotation connecting the nipple and its opposite point, the apex.

Motivated by that observation one might suspect that the spherical shape becomes unstable and that stability favours the oblong shape. In this section we show that that suspicion is unfounded, at least for a homogeneous Mooney-Rivlin balloon. So, whatever non-spherical shape is observed, it is either – most probably (!) – due to an inhomogeneity of thickness of the balloon membrane, or else the rubber of the balloon is not a Mooney-Rivlin material.

For a stability analysis of the spherical shape we must allow alternatives of shape for the inflated balloon, and for simplicity we permit shapes of rotational symmetry only.

### 9.2 A Modicum of Surface Geometry

Apart from the cartesian coordinates  $x_i = (x_1, x_2, x_3)$  we introduce cylindrical coordinates  $(\rho, \varphi, z)$  and surface coordinates  $U^\Delta = (\xi, \varphi)$ , cf. Fig. 9.1.

The  $x_3$ -axis is the axis of rotational symmetry and the origin of the cartesian coordinates is halfway between the poles, i.e. nipple and apex. The surface coordinate lines  $\varphi = \text{const}$  and  $\xi = \text{const}$  may be said to define longitudinal lines and parallels of latitude on the balloon, respectively. Thus point  $U^\Delta = (\xi, \varphi)$  on the balloon has the cartesian coordinates

$$x_i(U^\Delta) = \begin{bmatrix} \rho(\xi) \cos \varphi \\ \rho(\xi) \sin \varphi \\ z(\xi) \end{bmatrix}. \quad (9.1)$$

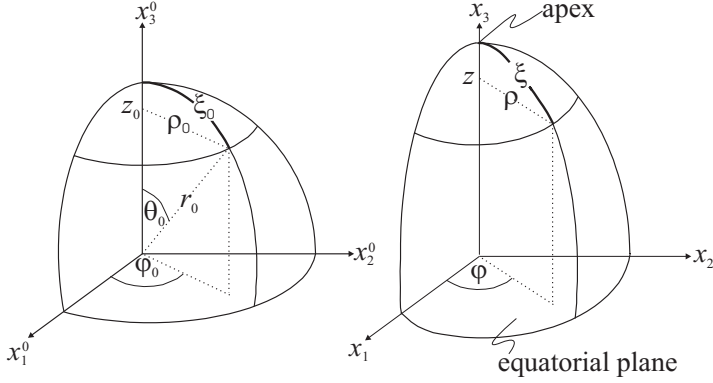


**Fig. 9.1.** Cartesian coordinates  $x_i = (x_1, x_2, x_3)$ , cylindrical coordinates  $(\rho, \varphi, z)$  and surface coordinates  $U^\Delta = (\xi, \varphi)$  in the undistorted state (left) and for the deformed balloon (right)

From these relations we determine all relevant surface properties:

**Tangential vectors**  $\tau_{i\Delta} = \frac{\partial x_i}{\partial U^\Delta}$  along the surface coordinate lines

$$\tau_{i\xi} = \begin{bmatrix} \frac{d\rho}{d\xi} \cos \varphi \\ \frac{d\rho}{d\xi} \sin \varphi \\ \frac{dz}{d\xi} \end{bmatrix}, \quad \tau_{i\varphi} = \begin{bmatrix} -\rho(\xi) \sin \varphi \\ \rho(\xi) \cos \varphi \\ 0 \end{bmatrix}. \quad (9.2)$$

**Metric tensor**  $g_{\Delta\Gamma} = \tau_{i\Delta} \tau_{i\Gamma}$  (note:  $d\xi^2 = dz^2 + d\rho^2$ )

$$g_{\Delta\Gamma} = \begin{bmatrix} 1 & 0 \\ 0 & \rho^2 \end{bmatrix}, \quad \text{hence} \quad g^{\Delta\Gamma} = \begin{bmatrix} 1 & 0 \\ 0 & \frac{1}{\rho^2} \end{bmatrix}. \quad (9.3)$$

**Christoffel symbols**  $\Gamma_{\Delta\Gamma}^\Sigma = \frac{1}{2} g^{\Sigma A} \left( \frac{\partial g_{\Delta A}}{\partial U^\Gamma} + \frac{\partial g_{A\Gamma}}{\partial U^\Delta} - \frac{\partial g_{\Delta\Gamma}}{\partial U^A} \right)$

$$\Gamma_{\varphi\varphi}^\xi = -\frac{1}{\rho} \frac{d\rho}{d\xi}, \quad \Gamma_{\xi\varphi}^\varphi = \Gamma_{\varphi\xi}^\varphi = \frac{1}{\rho} \frac{d\rho}{d\xi}, \quad \Gamma_{\Delta\Gamma}^\Sigma = 0 \quad \text{else.} \quad (9.4)$$

**Unit normal vector**  $n_i = \frac{\varepsilon_{ijk} \tau_j^\xi \tau_k^\varphi}{\sqrt{g}}$  on the surface;  $g$  is the determinant of  $g_{\Delta\Gamma}$

$$n_i = \begin{bmatrix} -\frac{dz}{d\xi} \cos \varphi \\ -\frac{dz}{d\xi} \sin \varphi \\ \frac{d\rho}{d\xi} \end{bmatrix}. \quad (9.5)$$

**Curvature tensor**  $b_{\Delta\Gamma} = \frac{\partial^2 x_i}{\partial U^\Delta \partial U^\Gamma} n_i$  of the surface

$$b_{\Delta\Gamma} = \begin{bmatrix} -\frac{1}{\sqrt{1-\left(\frac{d\rho}{d\xi}\right)^2}} \frac{d^2\rho}{d\xi^2} & 0 \\ 0 & \rho \sqrt{1-\left(\frac{d\rho}{d\xi}\right)^2} \end{bmatrix}.$$

### 9.3 Balance of Forces

The balance of forces in a point of the membrane requires that the divergence of the stress  $t_i^\Delta$  in the membrane equals the jump of pressure  $[p]$  across the membrane. We have

$$t_i^\Delta{}_{;\Delta} = [p]n_i, \quad (9.6)$$

where  $n_i$  is the unit normal on the membrane and the semicolon denotes the covariant derivative. Thus

$$t_i^\Delta{}_{;\Delta} = \frac{\partial t_i^\Delta}{\partial U^\Delta} + \Gamma_{\Sigma\Delta}^\Sigma t_i^\Delta. \quad (9.7)$$

$t_i^\Delta$  is the force in the direction  $x_i$  per line element on the membrane perpendicular to the coordinate line  $U^\Delta = \text{const}$ . This stress may be decomposed into tangential and normal components according to the relation

$$t_i^\Delta = S^{\Delta\Gamma} \tau_{i\Gamma} + S^\Delta n_i. \quad (9.8)$$

$S^\Delta$  represents a shear force which is equal to zero in a membrane and  $S^{\Delta\Gamma}$  are the contravariant components of the surface stress tensor.

We set  $S^\Delta = 0$  in (9.8) and use that relation in (9.6) to obtain – by use of the notions of Sect. 9.2 –

$$S^{\Delta\Gamma}{}_{;\Gamma} \tau_{i\Delta} + S^{\Delta\Gamma} b_{\Delta\Gamma} n_i = [p]n_i. \quad (9.9)$$

The semicolon again represents the covariant derivative so that in the present case we have

$$S^{\Delta\Gamma}{}_{;\Gamma} = \frac{\partial S^{\Delta\Gamma}}{\partial U^\Gamma} + \Gamma_{FA}^\Delta S^{A\Gamma} + \Gamma_{FA}^\Gamma S^{\Delta A}. \quad (9.10)$$

Equation (9.9) has two tangential components and one normal component. They read

$$S^{\Delta\Gamma}{}_{;\Gamma} g_{A\Delta} = 0 \quad \text{and} \quad S^{\Delta\Gamma} b_{\Delta\Gamma} = [p] \quad (9.11)$$

and they represent the balance of forces in the respective directions, or the equilibrium conditions for the balloon. Mathematically these equations will be seen to furnish the functional equations for the equilibrium shapes of the balloon.

## 9.4 Motion, Stretches, Surface Stress, and Pressure

A point on the balloon in the undistorted state is characterized by the cylindrical coordinates  $(\rho_0, \varphi_0, z_0)$  or by the surface coordinates  $(\xi_0, \varphi_0)$ . The motion of that point during a rotationally symmetric inflation may be written as

$$\rho = \rho(\rho_0, z_0), \quad \varphi = \varphi_0, \quad z = z(\rho_0, z_0). \quad (9.12)$$

$\varphi = \varphi_0$  expresses the expectation that the planes defined by the longitudinal lines are invariant under the inflation. The undistorted state is a sphere with the given radius  $r_0$ . Therefore  $\rho_0$  and  $z_0$  are not independent variables. We have

$$\rho_0 = r_0 \sin \frac{\xi_0}{r_0} \quad \text{and} \quad z_0 = r_0 \cos \frac{\xi_0}{r_0}, \quad (9.13)$$

so that the motion (9.12)<sub>1,3</sub> may be expressed as

$$\rho = \rho(\xi_0) \quad \text{and} \quad z = z(\xi_0). \quad (9.14)$$

Once the functions  $\rho = \rho(\xi_0)$  and  $z = z(\xi_0)$  have been determined, the shape of the balloon is known.

The stretches of the balloon in the directions of the surface coordinate lines are obviously

$$\lambda = \frac{d\xi}{d\xi_0} \quad \text{and} \quad \mu = \frac{\rho}{\rho_0} \quad (9.15)$$

and, by (3.19), the physical components of the surface stress tensor read<sup>1</sup>

$$\begin{aligned} S\langle 11 \rangle &= |s_-| \, d_0 \frac{1}{\lambda\mu} \left( \lambda^2 - \frac{1}{\lambda^2\mu^2} \right) (K + \mu^2), \\ S\langle 22 \rangle &= |s_-| \, d_0 \frac{1}{\lambda\mu} \left( \mu^2 - \frac{1}{\lambda^2\mu^2} \right) (K + \lambda^2). \end{aligned} \quad (9.16)$$

Thus only the diagonal components of the surface stress tensor are not equal to zero and the corresponding contravariant components are

$$S^{11} = S\langle 11 \rangle \, g^{11} = S\langle 11 \rangle, \quad S^{22} = S\langle 22 \rangle \, g^{22} = S\langle 22 \rangle \frac{1}{\rho^2}. \quad (9.17)$$

Taken altogether the last three equations determine the stresses in terms of the functions  $\rho = \rho(\xi_0)$ ,  $z = z(\xi_0)$ . We have from (9.15) and (9.16)

<sup>1</sup> Since  $S\langle 11 \rangle$  and  $S\langle 22 \rangle$  are forces per line element, they differ from  $t_{\lambda\lambda}$  and  $t_{\mu\mu}$  in (3.19) by the thickness  $d = d_o\nu = d_o \frac{1}{\lambda\mu}$  of the balloon.

$$\begin{aligned}
S\langle 11 \rangle &= |s_-| \, d_0 \frac{1}{\xi' \frac{\rho}{\rho_0}} \left( \xi'^2 - \frac{1}{\xi'^2 \left( \frac{\rho}{\rho_0} \right)^2} \right) \left( K + \left( \frac{\rho}{\rho_0} \right)^2 \right) \\
S\langle 22 \rangle &= |s_-| \, d_0 \frac{1}{\xi' \frac{\rho}{\rho_0}} \left( \left( \frac{\rho}{\rho_0} \right)^2 - \frac{1}{\xi'^2 \left( \frac{\rho}{\rho_0} \right)^2} \right) (K + \xi'^2),
\end{aligned} \tag{9.18}$$

where the prime here and in the sequel denotes differentiation with respect to  $\xi_0$ .

We also need the pressure difference  $[p] = p - p_0$  in terms of these functions. We recall that

$$[p] = \frac{NkT}{V} - p_0, \tag{9.19}$$

where  $V$  is the volume of the rotationally symmetric balloon, so that we may write

$$V = -\pi \int_0^\pi \rho^2 \frac{dz}{d\xi_0} d\xi_0. \tag{9.20}$$

## 9.5 Equilibrium Conditions

Combining the formulae of the previous three sections, namely,

- the knowledge about the surface geometry,
- the expectations about the type of non-spherical deformation, and
- the constitutive assumptions

we obtain for the conditions (9.11) of equilibrium.

Tangential component 1:

$$S' \langle 11 \rangle - \frac{1}{\rho} \rho' (S \langle 22 \rangle - S \langle 11 \rangle) = 0. \tag{9.21}$$

Tangential component 2: identically satisfied

Normal component:

$$\frac{1}{\sqrt{1 - \left( \frac{\rho'}{\xi'} \right)^2}} \frac{1}{\xi'} \left( \frac{\rho'}{\xi'} \right)' S \langle 11 \rangle - \frac{1}{\rho} \sqrt{1 - \left( \frac{\rho'}{\xi'} \right)^2} S \langle 22 \rangle = -[p]. \tag{9.22}$$

If we combine these equations with the explicit expressions (9.18) for the stress components and with the relations (9.19), (9.20) for the pressure jump, we obtain explicit field equations.

Inspection shows that these two equations form a coupled system of integro-differential equations for  $\rho(\xi_0)$  and  $\xi(\xi_0)$ . We consider the filling  $N$

as given. The system of equations becomes a system of differential equations only when  $[p]$  is given.

As natural boundary values we adopt the conditions

$$\rho(\xi_0 = 0) = 0, \quad \rho(\xi_0 = \pi r_0) = 0, \quad \xi(\xi_0 = 0) = 0, \quad (9.23)$$

so that the *poles remain poles* during the inflation. Also we expect that

$$z'(\xi_0 = 0) = 0 \quad \text{and} \quad z'(\xi_0 = \pi r_0) = 0, \quad (9.24)$$

so that the *balloon remains flat at the poles*.

It is an easy task to show that a spherical balloon of radius  $r$  satisfies the equilibrium conditions as well as the boundary values. In that case we set

$$\rho(\xi_0) = r \sin \frac{\xi_0}{r_0} \quad \text{and} \quad \xi(\xi_0) = \frac{r}{r_0} \xi_0, \quad (9.25)$$

and these functions satisfy (9.21) identically, whereas (9.22) implies

$$2|s_-| \frac{d_0}{r_0} \left( \frac{r_0}{r} - \left( \frac{r_0}{r} \right)^7 \right) \left( K + \left( \frac{r}{r_0} \right)^2 \right) = \frac{NkT}{\frac{4\pi}{3}r^3} - p_0, \quad (9.26)$$

which is – as it should be – the well-known pressure-radius relation for a spherical balloon, cf. (3.24).

## 9.6 Testing Stability of the Spherical Solution

In order to test the stability of the spherical solution we investigate a small deviation from sphericity, namely

$$\rho(\xi_0) = r \sin \frac{\xi_0}{r_0} + \hat{\rho}(\xi_0) \quad \text{and} \quad \xi(\xi_0) = \frac{r}{r_0} \xi_0 + \hat{\xi}(\xi_0). \quad (9.27)$$

Insertion into (9.21) and (9.22) and linearization in the small deviations  $\hat{\rho}$  and  $\hat{\xi}$  and their derivatives yields for the tangential component

$$\begin{aligned} & + \{2x^3 + x^4 + x^{10} + K(3x^2 + 2x^7 - x^8)\} \cos \vartheta_0 \hat{\rho}(\vartheta_0) + \\ & + \{-x^4 - x^{10} + K(-3x^2 + x^8)\} \sin \vartheta_0 \frac{d\hat{\rho}}{d\vartheta_0} + \\ & + \{-2x^3 - 2Kx^7\} \sin \vartheta_0 \cos \vartheta_0 \frac{d\hat{\xi}}{d\vartheta_0} + \\ & + \{-3x^4 - x^{10} + K(-3x^2 - x^8)\} \sin^2 \vartheta_0 \frac{d^2 \hat{\xi}}{d\vartheta_0^2} = 0, \end{aligned} \quad (9.28)$$

and for the normal component

$$\begin{aligned}
& \left\{ -5x^4 - x^{10} + K(-7x^2 + x^8) \right\} \hat{\rho}(\vartheta_0) + \\
& + \left\{ -6x^4 + K(-8x^2 + 2x^8) \right\} \sin \vartheta_0 \frac{d\hat{\xi}}{d\vartheta_0} + \\
& + \left\{ -x^4 + x^{10} + K(-x^2 + x^8) \right\} \frac{d^2 \hat{\rho}}{d\vartheta_0^2} + \\
& + \left\{ x^4 - x^{10} + K(x^2 - x^8) \right\} \cos \vartheta_0 \frac{d^2 \hat{\xi}}{d\vartheta_0^2} = \\
& = x^9 r_0 \sin \vartheta_0 \left( \frac{3}{2} \int_0^\pi \sin^2 \vartheta_0 \hat{\rho}(\vartheta_0) d\vartheta_0 + \frac{3}{4} \int_0^\pi \sin \vartheta_0 \frac{d\hat{\xi}}{d\vartheta_0} d\vartheta_0 - \frac{3}{4} \int_0^\pi \cos \vartheta_0 \frac{d\hat{\xi}}{d\vartheta_0} d\vartheta_0 \right). \tag{9.29}
\end{aligned}$$

Here we have abbreviated  $\frac{r}{r_0}$  by  $x$  and  $\frac{\xi_0}{r_0}$  by  $\vartheta_0$ , cf. Fig. 9.1.

The boundary conditions (9.23), (9.24) imply

$$\begin{aligned}
& \hat{\rho}(0) = 0, \quad \hat{\rho}(\vartheta_0 = \pi) = 0, \quad \hat{\xi}(0) = 0 \quad \text{and} \\
& \left. \frac{d\hat{\rho}}{d\vartheta_0} \right|_{\vartheta_0=0} = \left. \frac{d\hat{\xi}}{d\vartheta_0} \right|_{\vartheta_0=0}, \quad \left. \frac{d\hat{\rho}}{d\vartheta_0} \right|_{\vartheta_0=\pi} = - \left. \frac{d\hat{\xi}}{d\vartheta_0} \right|_{\vartheta_0=\pi}. \tag{9.30}
\end{aligned}$$

We decompose the solutions into harmonic modes of which each one satisfies the boundary conditions. Single modes for  $\hat{\rho}(\vartheta_0)$  and  $\hat{\xi}(\vartheta_0)$  are given by

$$\hat{\rho}_\alpha(\vartheta_0) = A_\alpha \cos \alpha \vartheta_0 + B_\alpha \sin \alpha \vartheta_0 \quad \text{and} \quad \hat{\xi}_\beta(\vartheta_0) = C_\beta \cos \beta \vartheta_0 + D_\beta \sin \beta \vartheta_0. \tag{9.31}$$

The boundary conditions (9.30)<sub>1,2,3</sub> require

$$A_\alpha = 0, \quad \alpha = n \ (n = 0, 1, 2, \dots), \quad \text{and} \quad C_\beta = 0.$$

Therefore mode  $n$  of  $\hat{\rho}(\vartheta_0)$  has the form

$$\hat{\rho}_n(\vartheta_0) = B_n \sin n \vartheta_0. \tag{9.32}$$

The boundary conditions (9.30)<sub>4,5</sub> imply

$$B_n n = D_\beta \beta \quad \text{and} \quad B_n n \cos n\pi = -D_\beta \beta \cos \beta\pi,$$

so that we obtain  $\beta = n + (2m + 1)$  with  $m = 0, 1, 2, \dots$ . A mode of  $\hat{\xi}(\vartheta_0)$  is thus characterized by a pair  $(n, m)$  and it reads

$$\hat{\xi}_{nm}(\vartheta_0) = B_n \frac{n}{n + 2m + 1} \sin(n + 2m + 1) \vartheta_0. \tag{9.33}$$

This mode is closely related to the  $n$ -mode of  $\hat{\rho}(\vartheta_0)$ ; in particular both are governed by the coefficient  $B_n$ .

Therefore the Fourier representation of the deviations  $\hat{\rho}(\vartheta_0)$  and  $\hat{\xi}(\vartheta_0)$  from the spherical shape read

$$\hat{\rho}(\vartheta_0) = \sum_{n=1}^{\infty} B_n \sin n\vartheta_0 \quad \text{and} \quad \hat{\xi}(\vartheta_0) = \sum_{n=1}^{\infty} \sum_{m=0}^{\infty} B_n \frac{n}{n+2m+1} \sin(n+2m+1)\vartheta_0. \quad (9.34)$$

The term for  $n = 0$  is omitted because it is trivially satisfied with  $\hat{\rho} = \hat{\xi} = 0$ .

We denote the curly brackets in (9.28) by  $A_1$  through  $A_4$  in the order of occurrence and insert the representations (9.34). After some rearrangement we thus obtain

$$\begin{aligned} & \sum_{n=0}^{\infty} \left\{ (A_1 - nA_2) \sin(n-1)\vartheta_0 + (A_1 + nA_2) \sin(n+1)\vartheta_0 - \right. \\ & - \sum_{m=0}^{\infty} [n(n+2m+1)A_4 \sin(n+2m+1)\vartheta_0 + \\ & + \left( \frac{n}{2}A_3 - \frac{n(n+2m+1)}{2}A_4 \right) \sin(n+2m-1)\vartheta_0 - \\ & \left. - \left( \frac{n}{2}A_3 - \frac{n(n+2m+1)}{2}A_4 \right) \sin(n+2m+3)\vartheta_0 \right\} B_n = 0. \end{aligned} \quad (9.35)$$

In particular the  $n$ -mode of  $\hat{\rho}$  and the  $(n, 0)$ -mode of  $\hat{\xi}$  must satisfy the relation

$$\begin{aligned} & \left\{ \left( A_1 - nA_2 - \frac{n}{2}A_3 + \frac{n(n+1)}{2}A_4 \right) \sin(n-1)\vartheta_0 \right. \\ & + (A_1 + nA_2 - n(n+1)A_4) \sin(n+1)\vartheta_0 + \\ & \left. + \frac{1}{2}(nA_3 + n(n+1)A_4) \sin(n+3)\vartheta_0 \right\} B_n = 0. \end{aligned} \quad (9.36)$$

For  $B_n$  to be unequal to zero its factor must vanish identically in  $\vartheta_0$ . This requires

$$\begin{aligned} A_1 - nA_2 - \frac{n}{2}A_3 + \frac{n(n+1)}{2}A_4 &= 0 \quad n > 1 \\ A_1 + nA_2 - \frac{n(n+1)}{2}A_4 &= 0 \quad n \geq 1 \\ nA_3 + n(n+1)A_4 &= 0 \quad n \geq 0. \end{aligned} \quad (9.37)$$

These are three algebraic equations for  $x$  – or two in case of  $n = 1$  – and it turns out that, for  $K = 10$ , there is no positive real solution for  $x$ . By (9.34) this means that  $B_n = 0$  holds, and that there is no alternative to the spherical balloon in the neighbourhood of the spherical shape. This follows



from (9.28) which represents the tangential component of the equilibrium condition. It is unnecessary to check the normal component (9.29) for non-trivial values of  $B_n$  since *both* components must be satisfied. On the other hand, obviously  $B_n = 0$  satisfies both components.

We conclude that the spherical shape of a Mooney-Rivlin balloon with  $K = 10$  is stable. At least there is no stable solution close to the spherical one so that no non-spherical shape can bifurcate off from the spherical one at any  $x$ .

## 9.7 Discussion

This simple result is somehow an anticlimax. Indeed, in order to obtain it, we bring to bear a fairly heavy analysis and out comes a somewhat bleak result: No instability of shape! However, we are not aware of a simpler method to derive that result and we did want to establish stability of the spherical shape. This is because doubts have been raised that a spherical balloon could be stable beyond a certain degree of inflation. Those doubts were based on the knowledge of the Kearsley instability of a flat membrane, cf. Chap. 4. Let us consider:

There is a paradox about the stability of the spherical shape of the balloon. Indeed, locally the balloon consists of little squares with equal loads on the sides and in Chap. 4 we have seen that such a situation is unstable beyond a critical stretch of  $\lambda = \mu = 3.17$ . So why is the balloon stable?

We cannot really put our finger on the essential difference between the balloon and the membrane. But we suggest that a small square cut out from the balloon may well behave differently from the same square firmly embedded in the balloon. After all, there are neighbouring squares to be taken into account in the latter case, and next-to-next neighbours as well. We recall that the shape of the balloon is governed by the integro-differential system (9.21), (9.22) with (9.18) and (9.19), (9.20).

In Sect. 9.1 we already remarked that balloons of non-spherical shape are often observed. From the result of the present chapter we must now conclude that either the rubber of such balloons is not of the Mooney-Rivlin type or the thickness  $d_0$  is not independent of  $\xi_0$ . The latter is the more likely cause of non-sphericity.

Indeed, most balloons are produced by dipping, i.e. a balloon-shaped mould is dipped into a liquid latex bath and a thin layer of latex – a rubber suspension, cf. Chap. 11 – sticks to the mould. It is inevitable that the latex flows to the bottom of the mould to some extent when it leaves the bath. Therefore all commercial balloons exhibit a discolouring at the apex or even a wart-like tubercle; the discolouring, or wart, is due to a greater thickness of the membrane at and around the apex. In contrast, the parts of the membrane close to the nipple are relatively thin.

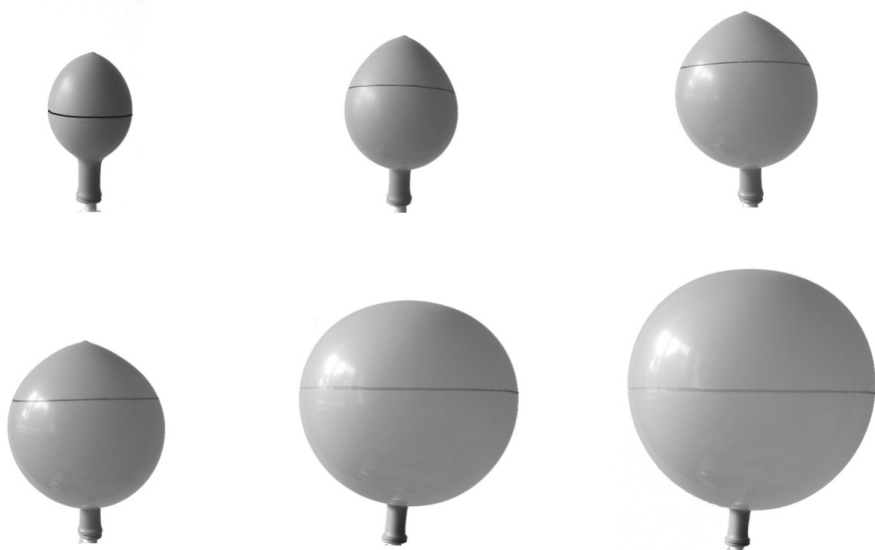


**Fig. 9.2.** Non-radial inflation of a balloon. A line is painted on the equator in the undistorted state

The variable thickness leads to a non-radial inflation of balloons which can easily be demonstrated by inflating a balloon whose “equator” has been marked by a painted circle before inflation, cf. Fig. 9.2<sub>upper left</sub>. Upon inflation this circle first moves forward and then backwards again, see Fig. 9.2.<sup>2</sup> It is true that none of the configurations in Fig. 9.2 is spherical, not even the undistorted one. Indeed, it is a rare occasion when a balloon is perfectly spherical and remains so upon inflation. Actually even the moulds are not spherical; rather they are mango-shaped.

---

<sup>2</sup> We saw this experiment – or a similar one – performed by A.N. Gent during an instructive course on non-linear continuum mechanics.